# The Solar Response Factor for the dynamic response of buildings to solar heat gains

**Gianpiero Evola – Department of Industrial Engineering, University of Catania – gevola@unict.it**
**Luigi Marletta – Department of Industrial Engineering, University of Catania – luigi.marletta@dii.unict.it**

## Abstract

The contribution of the solar heat gains to the cooling load is usually calculated through accurate procedures implemented in several simulation programs. Some simplified methods, such as the ASHRAE method, are also available for hand calculations, but they are based on tabular data that apply only to specific conditions.

This paper discusses a newly introduced parameter for the evaluation of the cooling load due to the solar radiation incident on the glazed surface of a building. This is the Solar Response Factor (SRF): it is a complex number, and can be rigorously defined and calculated as a combination of the thermal and the optical properties of walls and glazing.

In particular, the usefulness of the SRF is twofold. First, it allows us to classify the response of the enclosure to the solar radiation by means of a couple of parameters (amplitude and phase), which makes it easy to perform comparisons amongst different envelope solutions. Then, it allows for an easy analytical estimation of the cooling load in dynamic conditions, starting from the decomposition of the cyclic solar gains in a series of sinusoidal functions.

The paper discusses how the Solar Response Factor depends on the main thermo-physical and geometrical properties of the opaque and the glazed envelope. Moreover, an example is discussed to show how the use of the SRF allows us to evaluate the effectiveness of a series of solutions to limit the cooling load. The outcomes of this analysis provide very useful information for a conscious design of buildings, oriented to the limitation of the cooling load and the overheating of indoor spaces.

## 1. Introduction

In many buildings, the solar heat gains through the glazed envelope are a major portion of the total cooling load. However, it is not easy to estimate accurately these contributions, as they are transient in nature and due to thermal storage effects induced in the building mass.

Nowadays, several computer programs for the calculation of the cooling load are available. Most of them are based on the Heat Balance method (HB), which solves the problem rigorously, i.e. by calculating a conductive, convective, and radiative heat balance for each room surface, as well as a convective heat balance for the room air. As an example, the HB method is the basis of the BLAST (BLAST, 1991), the TARP (Walton, 1983) and the DOE-2 (York et al., 1980) energy analysis programs, implemented in several commercial software. However, the use of these programs implies a certain computational effort, as they require complex and very detailed input data concerning the building and the local weather conditions. This might be a problem for most designers, who tend to prefer a more straightforward and easy approach for the calculation of the cooling load.

Another approach for the cooling load calculation is the use of conduction transfer functions, as in the Transfer Function Method (TFM) (Mitalas, 1968). In this case, the time-varying response of the building, i.e. the cooling load, is related to the driving element, i.e. the weather data, through a series of transfer coefficients depending on the properties of the building envelope. Due to its user-friendliness, the TFM is a widely used computer-aided load calculation method in the air conditioning industry.

An approach similar to TFM is proposed in the Radiant Time Series method (RTS) (Spitler et al., 1997), which relies on a series of 24 response factors to compute conductive heat gains, and on a second series of 24 terms (the radiant time series)

to convert instantaneous radiant heat gains to cooling loads.

The research has also led to the definition of even simpler methods, to be used for manual calculation of the cooling load. In particular, in 1965 the *thermal storage factors* were defined – in the context of the Carrier method – as the ratio of the rate of instantaneous cooling load to the rate of solar heat gain (Carrier, 1965). The thermal storage factors have to be determined through appropriate tables depending on both the weight per unit floor area of the opaque components and the running time. Therefore, their use requires interpolation among tabular data; they are also rather rough, as they do not take into account the actual sequence of the wall layers, and they lack any theoretical basis, as they result from numerical simulations.

Similarly, the cooling load temperature difference (CLTD)/solar cooling load (SCL)/cooling load factor (CLF) method was more recently formulated (ASHRAE, 2009). Here, the space sensible cooling load from solar heat gains transmitted through the glazing can be calculated through a series of *solar cooling load factors* (SCL). ASHRAE has developed SCL values to be used for typical buildings in North America with weather data associated to July 21st at a latitude of 40°N. The accuracy of this approach is questionable for locations that are not placed at 40°N; in any case, up to now this cooling load calculation method has been widely used by HVAC designers.

In this paper, a substantially different approach is proposed. This approach is developed in the framework of the Admittance Procedure, a methodology built up in the early '70s, where the dynamic heat transfer through the opaque walls is assessed by means of the so-called *dynamic thermal properties* (Davies, 1973), (Millbank et al., 1974), (Loudon, 1970). In this context, a new parameter called the Solar Response Factor (SRF) has been recently introduced by the authors (Evola et al., 2013). The SRF is a complex number, quantified in terms of amplitude and phase; it is calculated as a combination of the thermal and the optical properties of walls and glazing. The use of the SRF allows managing analytically the calculation of the cooling load due to solar heat gains under steady-periodic conditions.

The reliability of this approach is successfully proven by comparison with a series of simulations carried out with EnergyPlus. Then, the paper discusses how the Solar Response Factor depends on the main thermo-physical and geometrical properties of the envelope. Finally, an example is presented to show how the use of the SRF allows us to evaluate the effectiveness of a series of solutions to limit the cooling load.

## 2. The Solar Response Factor

### 2.1 Definition and formulation

The rigorous calculation of the cooling load due to solar heat gains through the glazing is quite complex, as it involves several phenomena. Indeed, the solar radiation penetrating the glazing is firstly absorbed by the inner surface of the opaque envelope components. Then, the absorbed heat is partially transferred towards the indoor environment, due to the surface overheating: only the convective part of such thermal transfer contributes to the cooling load of the indoor space. Furthermore, in order to assess the cooling load, one must not forget the radiant energy absorbed by the glass itself and transferred by its inner surface to the indoor environment: this last component raises its importance as the glazed area increases.

All of these mechanisms are rigorously taken into account in the formulation of the *Solar Response Factor* SRF. This is defined as the overall convective heat flux released to the indoor air by all the inner surfaces of the envelope (walls plus glazing) per unit cyclic solar irradiance acting on the outer glazed surface. In formulae:

$$SRF = \frac{\sum_w \left( \tilde{q}_{w,c} \cdot A_w \right) + \sum_g \left( \tilde{q}_{g,c} \cdot A_g \right)}{\sum_g \left( \tilde{I}_g \cdot A_g \right)} \qquad (1)$$

It is important to remember that the formulation of the SRF is based on the concept of Surface Factor. According to the definition provided by (Millbank et al., 1974), this parameter quantifies the heat flux released by a wall to the environmental point per unit radiant heat gain collected on its inner surface, when the air temperatures on both sides of the wall

are held constant and equal, see Eq. (2). As discussed in (Evola and Marletta, 2013), the surface factor can be calculated through Eq. (3), where Y is the thermal admittance of the wall.

$$F = \frac{\tilde{q}_i}{\tilde{q}_{abs}}\bigg|_{\tilde{\theta}_i = \tilde{\theta}_o = 0} = \frac{\tilde{q}_i}{\alpha \cdot \tilde{\phi}} \qquad (2)$$

$$F = 1 - Y \cdot R_{si} \qquad (3)$$

Starting from these definitions, it is possible to derive an operational formulation for the SRF. The demonstration has already been presented in (Evola et al., 2013), and is here omitted. Eq. (4) reports this formulation in the case of an enclosure with only one window.

$$SRF = \frac{\sum_w\left(\alpha_{w,sw} \cdot F_w \cdot A_w \cdot h_{c,w} \cdot R_{si,w}\right)}{\left[\left(1-\rho_{g,sw}\right)\cdot f + \left(1-f\right)\cdot \bar{\alpha}_{w,sw}\right]\cdot A_{tot}} \cdot \tau_g + $$
$$+ 0.53\left(g_s - \tau_g\right)\cdot \frac{\sum_w\left(F_w \cdot A_w \cdot h_{c,w} \cdot R_{si,w}\right)}{A_{tot}} + 0.47\left(g_s - \tau_g\right) \qquad (4)$$

In Eq. (4), $f$ is a non-dimensional parameter, which measures the fraction of glazed surface to the overall surface of the enclosed space ($f = A_w / A_{tot}$). According to Eq. (4), the SRF depends on the optical properties of the envelope ($\alpha_w$, $\varrho_g$, $\tau_g$), as well as on the composition of the walls, which affects the calculation of the surface factors $F_w$.

Since the SRF depends on the Surface Factor, it results to be a complex number, characterized by an amplitude $|SRF|$ and a phase $\phi_{SRF}$.

## 2.2   Calculation of the cooling load

According to its definition, the usefulness of the SRF lies in the possibility of predicting the cooling load of a building due to solar heat gains, analytically and in the time domain.

To this aim, it is important to remember that any periodic function can be decomposed, by means of the Fourier analysis, in a series of sinusoidal functions, called *harmonics*, whose frequency is a multiple of the first harmonic, called *fundamental*.

Hence, the first step is the application of the Fourier analysis to the solar irradiance $I_g(t)$, in order to determine its mean value $I_{gm}$ and the harmonic components, up to the order $NH$ needed for a sufficient precision. The period of the $n$-th harmonics is $P_n = P/n$, where $P = 24$ h.

The second step is the calculation of the Solar Response Factor for the enclosure, see Eq. (4). This operation has to be repeated for each harmonic component: in this case, the surface factors $F_n$ have to be calculated with reference to the period $P_n$. It is also necessary to determine the stationary Solar Response Factor ($SRF_s$): it is a real number obtainable through the same relations as those used for SRF, but using the thermal transmittance U in place of the thermal admittance Y.

Finally, the time profile of the cooling load due to solar heat gains can be assessed through Eq. (5), where the harmonic components of the response are summed up to the order $NH$.

$$Q_c(t) = A_g \cdot \left[SRF_s \cdot I_{gm} + \sum_{n=1}^{NH}\left|SRF_n\right|\left|\tilde{I}_{gn}\right|\cos\left(\frac{2\pi t}{P_n} + \varphi_{SRFn}\right)\right] \quad (5)$$

The reliability of this approach is verified in the following section, based on the comparison with the results obtained through accurate and well-established methods.

## 3.   Validation of the proposed approach

In order to verify the reliability of the formulation proposed in Section 2 to calculate the cooling load due to solar radiation, a preliminary validation is performed. This is based on the comparison between the results of Eq. (5) and those obtained with accurate simulations on EnergyPlus for a simple test room, whose size is $5 \times 5 \times 3$ m³. As far as the envelope of the test room is concerned, four different building typologies are considered:

- *Case A*: heavy masonry walls (stone walls);
- *Case B.1*: double-leaf cavity walls with the insulation placed in the air gap;
- *Case B.2*: double-leaf cavity walls with the insulation placed on the inner side of the wall;
- *Case C*: single leaf lightweight clay walls.

The details concerning the composition of walls, floors and ceilings are reported in the Appendix, where the values of the corresponding surface factors F are also provided. In the calculation, two walls are considered as external walls, whereas the others look like internal walls. In any case, all opaque surfaces have the same short-wave absorptance ($\alpha_{sw} = 0.3$).

Furthermore, the room is equipped with a window, whose size is $A_g$ = 5.5 m², which corresponds to $f$ = 0.05. The window has double glazing filled with air ($U_g$ = 2.9 W m⁻² K⁻¹). In the calculation of SRF, no obstruction or shadings are considered.

For each type of envelope, four different simulations are carried out, to investigate all the possible exposures of the glazing. The optical properties of the double glazing, used in the calculation of the SRF, are reported in Table 1. They are determined through UNI EN 410:2011, and taking into account the average angle of incidence for each orientation. The weather data are those available on EnergyPlus for Catania (southern Italy).

Furthermore, it should be remembered that no forcing condition other than the solar radiation incident on the glazing must be taken into account in this context, according to the definition framework of both the *surface factor F* and the *solar response factor* SRF. For this reason, in the simulations with EnergyPlus a constant air temperature was imposed in the test room ($\theta_i$ = 26°C), and all the envelope elements were considered adjacent to other rooms with the same temperature.

Finally, Table 2 shows the values retained for $h_c$ and $R_{si}$. As already discussed in a previous work by the authors (Evola and Marletta, 2013), these values are different from those usually adopted by international standards. This position derives from the specific definition framework of SRF, which implies a certain homogenization of the inner surface temperatures. Consequently, a lower rate of surface-to–air convective and reciprocal radiant heat transfer is expected if compared to an "ordinary" situation.

Table 1 – Average optical properties of the glazing

|  | Glazing type | South | East/West | North |
|---|---|---|---|---|
| $\tau_g$ | Single | 0.647 | 0.748 | 0.719 |
|  | Double | 0.472 | 0.588 | 0.588 |
|  | Double reflective | 0.243 | 0.305 | 0.290 |
| $g_s$ | Single | 0.674 | 0.774 | 0.744 |
|  | Double | 0.547 | 0.663 | 0.633 |
|  | Double reflective | 0.363 | 0.425 | 0.410 |

Table 2 – Values retained for hc and Rsi

|  | Ceiling | Floor | Walls |
|---|---|---|---|
| $h_c$  [W·m⁻²·K⁻¹] | 1.0 | 1.2 | 1.4 |
| $R_{si}$  [m²·K·W⁻¹] | 0.9 | 0.75 | 0.65 |

Table 3 – Amplitude and phase of SRF for the test room (double glazing, $\alpha_{sw}$ = 0.3, f = 0.05)

|  |  | South | East/West | North |
|---|---|---|---|---|
| \|SRF\| [-] | Case A | 0.080 | 0.091 | 0.088 |
|  | Case B.1 | 0.140 | 0.165 | 0.158 |
|  | Case B.2 | 0.174 | 0.207 | 0.198 |
|  | Case C | 0.146 | 0.173 | 0.166 |
| $\phi_{SRF}$ [h] | Case A | 1.82 | 1.97 | 1.94 |
|  | Case B.1 | 1.99 | 2.08 | 2.03 |
|  | Case B.2 | 1.60 | 1.67 | 1.65 |
|  | Case C | 1.80 | 1.88 | 1.86 |

The amplitude |SRF| and the phase $\phi_{SRF}$ for the test room, calculated through Eq. (4) for all the exposures and all the envelope typologies, are shown in Table 3. Here, it is possible to observe that massive walls (Case A) imply lower amplitude |SRF| than in the other cases, thanks to their high inertia. Hence, a lower cooling load is expected. The difference between the building solutions is less pronounced when looking at $\phi_{SRF}$, which is always close to 2 h. Furthermore, placing the insulation layer close to the indoor environment (case B.2) determines the worst performance, with the highest values of |SRF| for all the exposures.

As far as the comparison between the proposed methodology and the results obtained with EnergyPlus is concerned, the outcomes are shown in Fig. 1. The comparison is based both on the peak cooling load (Fig. 1a) and the daily energy demand (Fig. 1b), i.e. the time integral of the cooling load over a daily period. In order to calculate the cooling load, *NH* = 6 has been set in Eq. (5); the introduction of further harmonics would not modify the result.

The discrepancy on both parameters never exceeds 10%, and actually rarely exceeds 5%. The outcome of the validation is very satisfactory, given that quite a large window area is considered ($A_g$ = 5.5 m²): even better results were obtained in the case of an enclosure with smaller windows.

Another interesting result is shown in Fig. 2. Here, one can observe that $NH = 3$ is sufficient to produce a reliable profile of the cooling load. Indeed, the highest discrepancy between $NH = 3$ and $NH = 6$ is around 2% on the peak cooling load. Similar results are obtained for other envelope solutions.
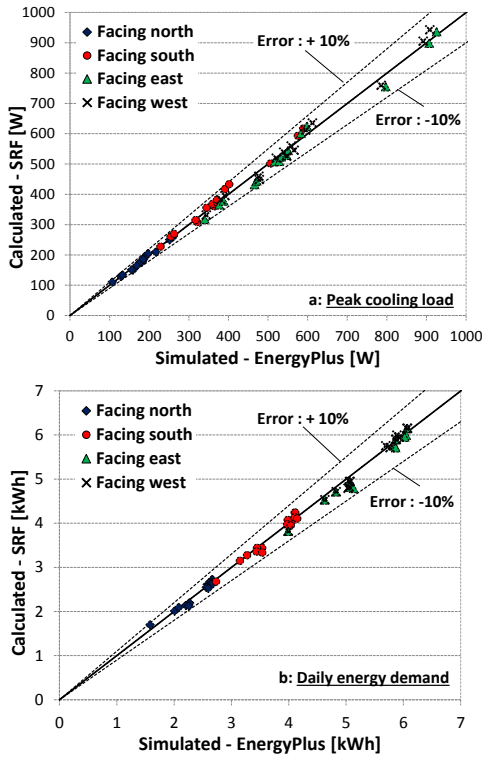


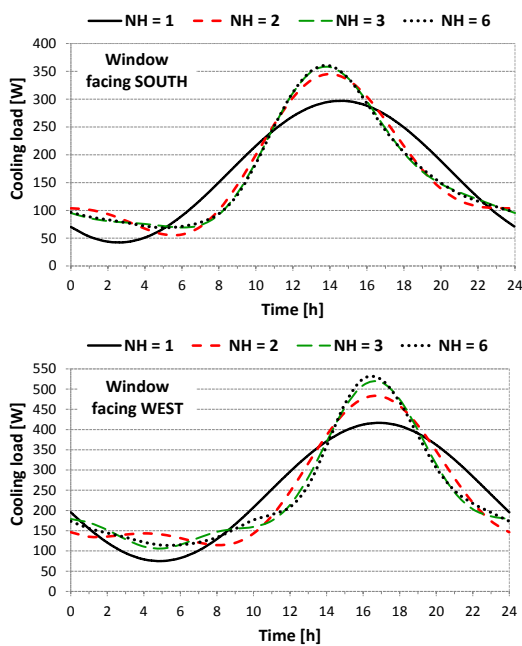Fig. 1 – Discrepancy between calculated and reference results



Fig. 2 – Summation of the harmonics in Eq. 5 (case B.1)

## 4. Parametric analysis

In this section, the paper discusses how the SRF depends on the glazing type, the size of glazed surface – described through the non-dimensional parameter $f$ – and the solar absorptance $\alpha$ of the inner surfaces. Here, three different glazing solutions are considered, i.e. single glazing, double glazing and double glazing with a reflective outer pane; the average optical properties for all typologies are those listed in Table 1.

The amplitude $|SRF|$ and the phase $\phi_{SRF}$ of the Solar Response Factor, calculated through Eq. (4) for several combinations of these parameters, are reported in Fig. 3. The calculation is extended to all the envelope solutions and the window exposures.
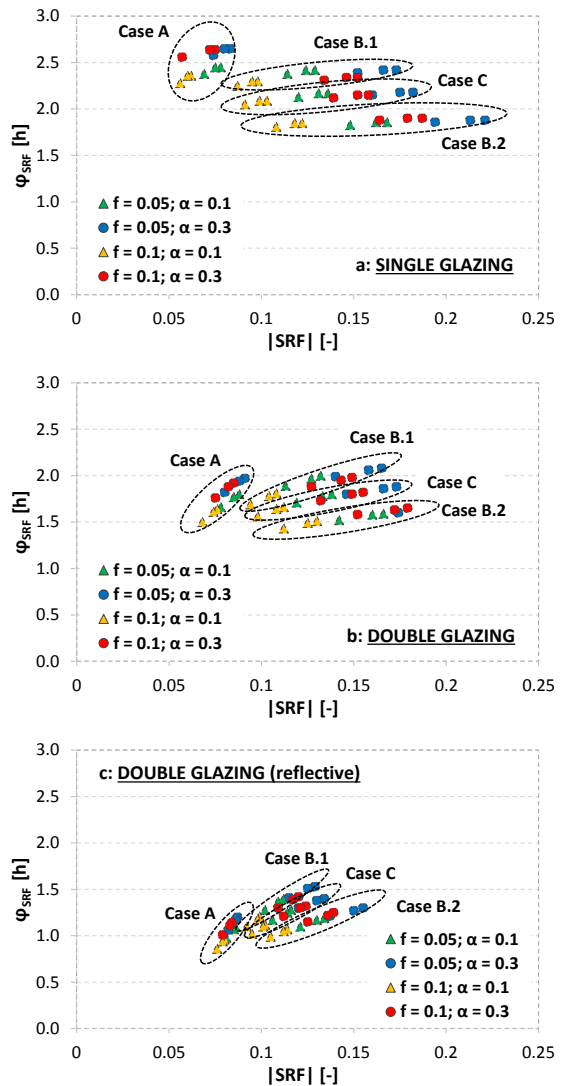


Fig. 3 – The Solar Response Factor of the sample room for different glazing types and size

As is possible to observe, the use of a reflective glazing tends to reduce the differences between the envelope solutions, since the solar gains are significantly cut by the glazing itself. Hence, the thermal inertia of the opaque envelope has a lower importance. A reflective glazing yields lower |SRF| than common double glazing. However, the phase is also lower, due to the higher rate of solar irradiance absorbed by the glazing, and then transferred by convection to the indoors.

## 5. Useful application of the SRF

The SRF can also be conveniently used to perform comparisons between different strategies for the reduction of the cooling load.

As an example, let us consider the test room described in Section 3. Starting from the configuration already introduced (double glazing, $\alpha$ = 0.3, f = 0.05), which is identified as the "base case" in the following, several potential strategies are suggested to reduce the cooling load, namely:

- Outer reflective pane on the window;
- Low absorptance of the inner surface ($\alpha$ = 0.2);
- Installation of an insulating layer (40 mm of polystyrene) either on the inner or on the outer side of the external wall.

Hence, for each proposed intervention, the SRF of the room is calculated through Eq. (4), and the daily profile of the cooling load is determined by means of Eq. (5). This analysis is applied to Case A and Case C, with reference to a window due south. The results are shown in Fig. 4. Here, we can observe that the application of an insulation layer on the outer wall is not a good idea. In particular, placing the insulation on the inner side significantly increases the peak cooling load, especially in Case A, where the detrimental effect on the thermal inertia of the wall is more pronounced. In case C, placing the insulation on the outer side has no effect on the cooling load.

On the other hand, the use of a lighter inner plaster ($\alpha$ = 0.2) has a positive effect, as expected. However, the reduction of the peak cooling load due to this intervention is not significant. The best solution consists in the use of a reflective pane on the outer side of the window.
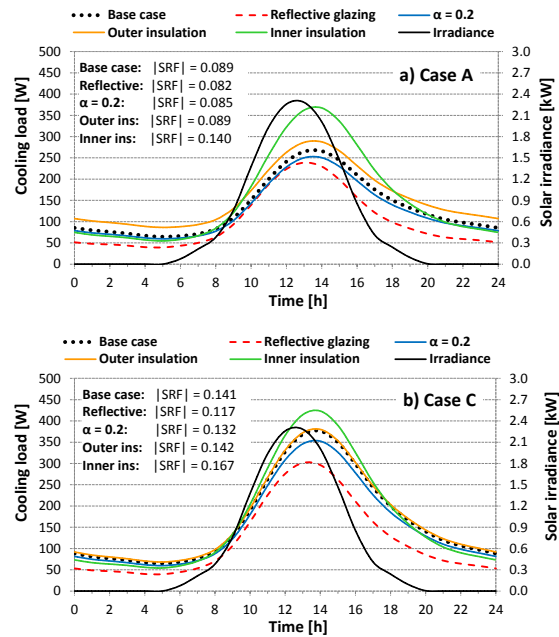


Fig. 4 – Cooling load of the test rom for different configurations.

In any case, the same conclusions about the effectiveness of such strategies could be foreseen from the values of |SRF| reported in the graphs of Fig. 4. Indeed, the higher |SRF|, the higher the resulting peak cooling load.

## 6. Conclusion

The Solar Response Factor proves to be very useful to assess the energy performance of buildings.

The main quality of the SRF is that it represents a transfer function of the whole enclosure in relation to solar excitations, in the form of a single complex number. Its formulation is derived analytically, and involves all the thermo-physical properties of the envelope.

The SRF can be used to make comparisons between different building solutions in the design stage, or to classify existing buildings in relation to their capacity to attenuate the effects of solar radiation, without the need of complex dynamic simulations.

If compared to the Solar Cooling Load factor (SCL) defined by Ashrae, the SRF shows solid theoretical bases and is more general and rigorous.

For all these reasons, the use of the SRF can be recommended to professionals and researchers as a very useful tool to evaluate the response of buildings to solar heat gains.

## 7. Nomenclature

### Symbols

| | |
|---|---|
| A | area ($m^2$) |
| f | fraction of glazed surface (-) |
| F | surface factor (-) |
| $g_s$ | glass g-value (-) |
| h | heat transfer coefficient (W $m^{-2}$ $K^{-1}$) |
| I | solar irradiance (W $m^{-2}$) |
| n | order of the harmonic (-) |
| NH | total number of harmonics (-) |
| P | time period (h) |
| q | density of heat flux (W $m^{-2}$) |
| $Q_c$ | cooling load (W) |
| R | thermal resistance ($m^2$ K $W^{-1}$) |
| SRF | solar response factor (-) |
| U | thermal transmittance (W $m^{-2}$ $K^{-1}$) |
| Y | thermal admittance (W $m^{-2}$ $K^{-1}$) |

### Greek letters

| | |
|---|---|
| $\alpha$ | absorptance (-) |
| $\rho$ | reflectance (-) |
| $\tau$ | transmittance (-) |
| $\phi$ | time shift (h) |
| $\varphi$ | radiant heat flux (W $m^{-2}$) |

### Subscripts/Superscripts

| | |
|---|---|
| abs | absorbed |
| c | convective |
| g | glazing |
| h | harmonic |
| i | indoor |
| o | outdoor |
| si | inner surface |
| sw | short-wave |
| w | wall |

### References

ASHRAE, American Society of Heating, Refrigerating and Air Conditioning Engineers. 2009. "Chapter 18: Nonresidential cooling and heating load calculations". In *ASHRAE Handbook of Fundamentals,* edited by ASHRAE.

BLAST Support Office. 1991. *BLAST user reference.* Urbana Champaign: University of Illinois.

Carrier Air Conditioning Co. 1965. *Handbook of Air Conditioning System Design (1st ed.).* New York: McGraw-Hill.

CIBSE. 2006. *Environmental Design CIBSE Guide A.* London: The Yale Press Ltd.

Davies M. G. 1994. "The thermal response of an enclosure to periodic excitation: the CIBSE approach". *Building and Environment* 29 (2): 217-235. doi:10.1016/0360-1323(94)90072-8.

EN 410:2011. "Glass in building – Determination of luminous and solar characteristics of glazing".

Evola G., Marletta L. 2013. "A dynamic parameter to describe the thermal response of buildings to radiant heat gains". *Energy and Buildings* 65: 448-457. doi:10.106/j.enbuild.2013.06.026.

Evola G., Marletta L., Sicurella F. 2013. "A dynamic parameter for dealing with solar gains in buildings". In *Proceedings of Building Simulation 2013*, edited by Etienne Wurtz, 161-168.

ISO 13792:2012. "Thermal performance of buildings – Calculation of internal temperatures of a room in summer without mechanical cooling – Simplified methods".

Loudon A. G. 1970. "Summertime temperatures in buildings without air conditioning". *Journal of the Institution of Heating and Ventilation Engineers* 37: 280-292.

Millbank N. O., Harrington-Lynn J. 1974. "Thermal response and the admittance procedure". *Building Service Engineering* 42: 38-51.

Mitalas G. P. 1968. "Calculation of transient heat flows through walls and roofs" in *ASHRAE Transactions* 74 (2): 182-188.

Spitler J. D., Fisher D. E., Pedersen C. O. 1997. "The radiant time series cooling load calculation procedure" in *ASHRAE Transactions* 103 (2): 503-515.

Walton G. 1983. *Thermal Analysis Research Program reference manual.* National Bureau of Standards.

York D. A., Tucker E. F., Cappiello C. C. 1980. *DOE-2 engineers manual (Version 2.1A).* Lawrence Berkeley Laboratory and Los Alamos National Laboratory.

**External wall: Case A**

| Material | s [m] | |F| [-] | φF [h] | U [W/m²K] |
|---|---|---|---|---|
| Inner plaster | 0.01 | | | |
| Lava stones | 0.60 | 0.086 | 2.3 | 1.90 |
| Outer plaster | 0.01 | | | |

**External wall: Case B.1**

| Material | s [m] | |F| [-] | φF [h] | U [W/m²K] |
|---|---|---|---|---|
| Inner plaster | 0.01 | | | |
| Hollow clay bricks | 0.08 | | | |
| Air cavity | 0.03 | | | |
| Polystyrene | 0.05 | 0.318 | 3.5 | 0.35 |
| Hollow clay bricks | 0.25 | | | |
| Outer plaster | 0.01 | | | |

**External wall: Case B.2**

| Material | s [m] | |F| [-] | φF [h] | U [W/m²K] |
|---|---|---|---|---|
| Inner plaster | 0.01 | | | |
| Polystyrene | 0.05 | | | |
| Hollow clay bricks | 0.08 | | | |
| Air cavity | 0.03 | 0.644 | 1.6 | 0.35 |
| Hollow clay bricks | 0.25 | | | |
| Outer plaster | 0.01 | | | |

**External wall: Case C**

| Material | s [m] | |F| [-] | φF [h] | U [W/m²K] |
|---|---|---|---|---|
| Inner plaster | 0.01 | | | |
| Light bricks | 0.38 | 0.364 | 2.5 | 0.35 |
| Outer plaster | 0.01 | | | |

**Internal partitions: Case A**

| Material | s [m] | |F| [-] | φF [h] | U [W/m²K] |
|---|---|---|---|---|
| Inner plaster | 0.01 | | | |
| Lava stones | 0.40 | 0.084 | 2.2 | 1.66 |
| Outer plaster | 0.01 | | | |

**Internal partitions: <u>Case B + Case C</u>**

| Material | s [m] | |F| [-] | $\phi_F$ [h] | U [W/m²K] |
|---|---|---|---|---|
| Inner plaster | 0.01 | | | |
| Hollow clay bricks | 0.08 | 0.305 | 2.3 | 0.89 |
| Outer plaster | 0.01 | | | |

**Floor: <u>Case A</u>**

| Material | s [m] | |F| [-] | $\phi_F$ [h] | U [W/m²K] |
|---|---|---|---|---|
| Concrete tiles | 0.01 | | | |
| Lean concrete | 0.06 | | | |
| Pumice/gypsum | 0.12 | 0.150 | 3.8 | 0.75 |
| Inner plaster | 0.01 | | | |

**Table 8 – Floor: <u>Case B + Case C</u>**

| Material | s [m] | |F| [-] | $\phi_F$ [h] | U [W/m²K] |
|---|---|---|---|---|
| Concrete tiles | 0.01 | | | |
| Lightweight screed | 0.05 | | | |
| Concrete-slabs flooring | 0.20 | 0.260 | 2.2 | 0.92 |
| Inner plaster | 0.01 | | | |

**Ceiling: <u>Case A</u>**

| Material | s [m] | |F| [-] | $\phi_F$ [h] | U [W/m²K] |
|---|---|---|---|---|
| Inner plaster | 0.01 | | | |
| Pumice/gypsum | 0.12 | | | |
| Lean concrete | 0.06 | 0.296 | 2.8 | 0.30 |
| Concrete tiles | 0.01 | | | |

**Ceiling: <u>Case B + Case C</u>**

| Material | s [m] | |F| [-] | $\phi_F$ [h] | U [W/m²K] |
|---|---|---|---|---|
| Inner plaster | 0.01 | | | |
| Concrete-slabs flooring | 0.20 | | | |
| Polystyrene | 0.05 | 0.112 | 2.6 | 0.11 |
| Lightweight screed | 0.05 | | | |
| Concrete tiles | 0.01 | | | |